Los Alamos NATIONAL LABORATORY EST.1943

LA-UR-14-24792 (Accepted Manuscript)

Handheld Readout Electronics to Fully Exploit the Particle Discrimination Capabilities of Elpasolite Scintillators

Budden, Brent S.; Stonehill, Laura C.; Warniment, Adam; Michel, John M.; Storms, Steven A.; Dallmann, Nicholas; Coupland, Daniel D.; Stein, Paul S.; Weller, Stephen L.; Borges, Louis; Proicou, Michael C.; Duran II, Melvin G.; Kamto, Joseph

Provided by the author(s) and the Los Alamos National Laboratory (2016-02-11).

To be published in: Nuclear Instruments and Methods in Physics Research, Section A: Accelerators, Spectrometers, Detectors and Associated Equipment ; Vol.795, p.213-218, 21 September 2015

DOI to publisher's version: 10.1016/j.nima.2015.06.004

Permalink to record: http://permalink.lanl.gov/object/view?what=info:lanl-repo/lareport/LA-UR-14-24792

Disclaimer:
Approved for public release. Los Alamos National Laboratory, an affirmative action/equal opportunity employer, is operated by the Los Alamos National Security, LLC for the National Nuclear Security Administration of the U.S. Department of Energy under contract DE-AC52-06NA25396. Los Alamos National Laboratory strongly supports academic freedom and a researcher's right to publish; as an institution, however, the Laboratory does not endorse the viewpoint of a publication or guarantee its technical correctness.

RESEARCH LIBRARY

Handheld Readout Electronics to Fully Exploit the Particle Discrimination Capabilities of Elpasolite Scintillators

B. S. Budden[a,*], L. C. Stonehill[a], A. Warniment[a], J. Michel[a], S. Storms[a], N. Dallmann[a], D. D. S. Coupland[a], P. Stein[a], S. Weller[a], L. Borges[a], M. Proicou[a], G. Duran[a], J. Kamto[a,b]

[a] *Intelligence and Space Research Division, Los Alamos National Laboratory, Los Alamos, NM 87545 USA*
[b] *Electrical & Computer Engineering Department, Praire View A&M University, Prairie View, TX 77446 USA*

Abstract

A new class of elpasolite scintillators has garnered recent attention due to the ability to perform as simultaneous gamma spectrometers and thermal neutron detectors. Such a dual-mode capability is made possible by pulse-shape discrimination (PSD), whereby the emission waveform profiles of gamma and neutron events are fundamentally unique. To take full advantage of these materials, we have developed the Compact Advanced Readout Electronics for Elpasolites (CAREE). This handheld instrument employs a multi-channel PSD-capable ASIC, custom micro-processor board, front-end electronics, power supplies, and a 2" photomultiplier tube for readout of the scintillator. The unit is highly configurable to allow for performance optimization amongst a wide sample of elpasolites which provide PSD in fundamentally different ways. We herein provide an introduction to elpasolites, then describe the motivation for the work, mechanical and electronic design, and preliminary performance results.

Keywords: Elpasolite, CLYC, Handheld, Pulse Shape Discrimination, Scintillator

*Corresponding author
Email address: bbudden@lanl.gov (B. S. Budden)

1. Introduction

A new class of Cerium-doped elpasolite scintillators has garnered recent attention due to the ability to perform as dual-mode detectors: gamma spectroscopy is complemented by thermal neutron detection via the ^{6}Li(n_{th},α)T capture reaction. Examples of such scintillators include Cerium-doped Cs_2LiYCl_6 (CLYC), $Cs_2LiLaBr_6$-Cl (CLLB-C), Cs_2LiYBr_6 (CLYB), and $Cs_2LiLaCl_6$ (CLLC). Gamma and neutron events may be uniquely identified by pulse-shape discrimination (PSD), which is made feasible due to unique emission waveforms arising from the incident particle interactions within the crystal.

The most popular of these scintillators is arguably CLYC, with recent commercialization of 1"-right crystals, thorough investigations into its scintillation mechanisms and PSD performance [1, 2, 3, 4, 5], and implementation in many novel dual-mode gamma spectrometers and neutron counters (e.g., [6, 7]). It emits at a peak wavelength of 390 nm that is well-matched to many commercial photomultiplier tubes (PMTs), has a density of 3.31 g/cm^3, and exhibits better energy resolution than commonly-used NaI crystals [8]. Part of the success of CLYC and other chloro-elpasolites is due to the excellent PSD performance, for which the ultrafast decay from core-valence luminescence (CVL) [9] in gamma-induced scintillation is mostly responsible. The other elpasolites have garnered less attention due to the complete absence of CVL in all interactions, although PSD is still achieved due to a difference in the fraction of slower emission mechanisms. Some of these other crystals exhibit better performance in other important applications, however. CLLB, for example, is one of the brightest elpasolites, providing up to 55 photons per keV of gamma energy to produce a resolution of 2.9% FWHM at 662 keV. CLLB may also be more suitable for use with solid state photodetectors, for which its scintillation wavelength of 410 nm is better matched than other elpasolites [10, 11, 12]. Although a bromide, the introduction of chlorine in CLLB-C also enables fast neutron sensitivity, as has been shown recently with CLYC [13, 14].

The various PSD performances, densities, light yields, and wavelength emis-

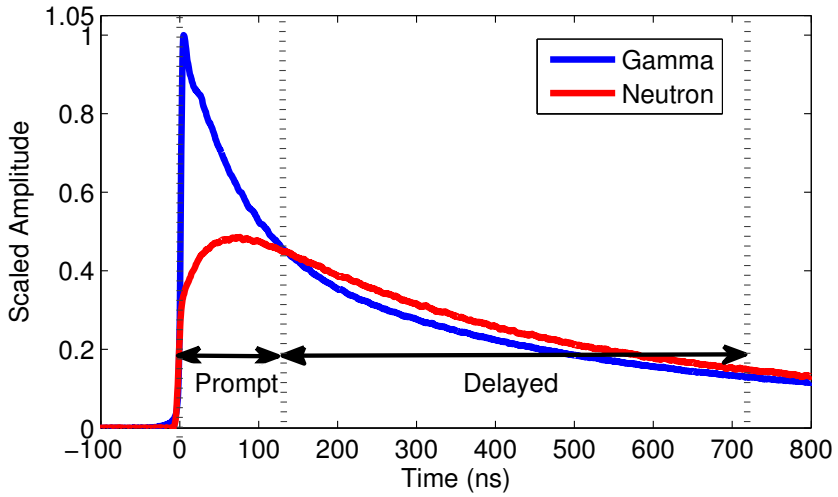

Figure 1: CLYC waveforms from gamma and neutron events with prompt and delayed integration windows indicated.

sions of elpasolites thus provide a range of suitable detectors for an assortment of applications. This variety is the motivation behind the development of handheld instrumentation capable of gamma spectroscopy and neutron detection that is highly configurable to enable optimized readout of any of the elpasolites. Such a device is of importance to first responders, border security agents, emergency personnel, and law enforcement agencies. In addition to hardware development, a significant portion of the effort has been in developing the concepts and algorithms necessary for its optimal functionality.

2. Pulse-Shape Discrimination in Elpasolites

Pulse shape discrimination is feasible with Chloro-elpasolites due to the presence of the ultrafast CVL emission in waveforms resulting from incident gammas. For Bromo-elpasolites, CVL is absent even in gamma interactions, though the emission waveforms due to gammas versus neutrons are still unique, and thus these crystals are also PSD-capable. To achieve PSD, we employ a tail-to-total

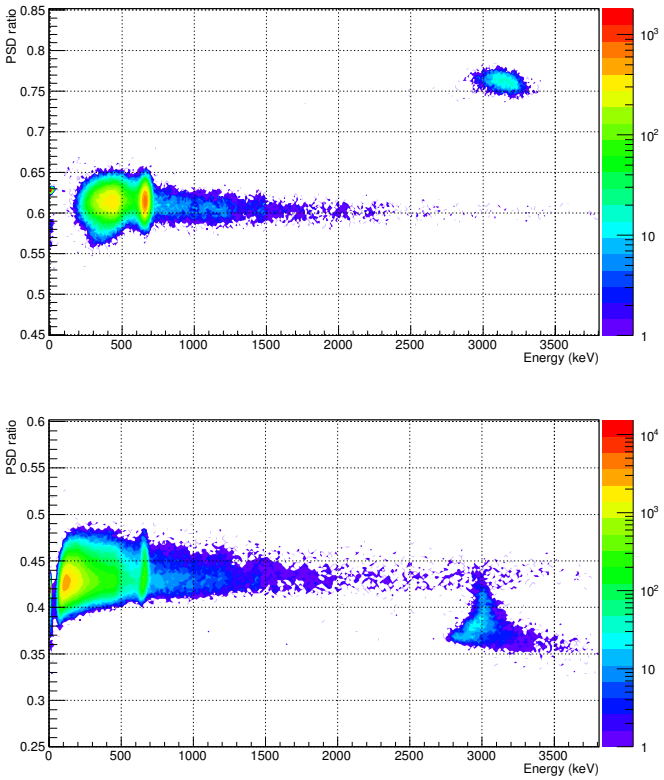

Figure 2: Plots of PSD ratio versus incident energy for (top) CLYC and (bottom) CLLB-C using a PSD-capable ASIC demonstrate the unique location of thermal neutrons for different elpasolites (seen as regions separate from a horizontal band of gammas). Here, data are shown from measurements of ^{137}Cs and ^{241}AmB sources.

ratio, R, calculated as

$$R = \frac{D}{P + D}, \tag{1}$$

where P and D are the integrated values of a prompt and delayed region of the waveform, respectively (see Fig. 1). For our purposes, the prompt windows commence at trigger time and the delayed window starts immediately after the end of the prompt integration. For optimal peformance, the window widths must be determined for the particular crystal, since the waveform shapes are dependent on material, doping concentration, quality, and size. A system gen-

erally applicable for use with all elpasolites (or more strictly, even for multiple samples of the same material), therefore, must not fix these values. Furthermore, to achieve good energy resolution, a third total integration window must be used for energy measurement and typically extends past the end of the delayed window, with a time dependent on the longest of the decay mechanisms for a particular scintillator.

On an event-by-event basis, these PSD ratios may be plotted against gamma-equivalent energy (GEE), producing a two-dimensional plot such as those in Fig. 2. In this figure, data are acquired from ^{137}Cs (γ) and ^{241}AmB ($\gamma + \mathrm{n}$) sources using custom electronics with the same PSD-capable ASIC as described in Sec. 3. The top plot shows results using CLYC; a horizontal band of gammas exists across a range of energies below a small region at higher PSD ratio. This region indicates the presence of thermal neutrons due to the slower decay constants of these waveforms. The Q-value of ^{6}Li capture reaction is 4.78 MeV; due to moderate quenching of the scintillation from heavy charged particles [15], the thermal neutron peak shows up at a GEE of 3.2 MeV [8]. A selection on this region of interest (by applying thresholds on both PSD ratio and energy) selects these events. The plot at the bottom of Fig. 2 shows results using CLLB-C. Here, the neutron waveforms decay faster than gammas, indicated by a lower ratio, with a GEE of 3.0 MeV [16]. Thus, it becomes obvious that the bounds of this region of interest must also be configurable for a general elpasolite readout instrument.

3. Electronics

The Compact Advanced Readout Electronics for Elpasolites (CAREE) is a handheld radiation detection instrument capable of simultaneous gamma spectroscopy and thermal neutron counting by employing any of the PSD-capable elpasolite scintillators. At the heart of the instrument is a custom ASIC known as the PSD8C [17]. The PSD8C is a charge integrating device, with three integrations occuring simultaneous on up to eight channels (here, we have used

only one). The ASIC is highly configurable, whereby input lines may be used to set window width and delays, signal offsets, integration gain, and more. The ASIC is thus ideally suited to the task of elpasolite PSD, providing the delayed, prompt, and total integration windows described in Sec. 2.

A field-programmable gate array (FPGA) communicates directly with the ASIC. For initial configuration the FPGA generates a master reset for the ASIC and sends a 48-bit configuration word to the ASIC via serial link. The FPGA then controls the ASIC through discrete digital input/output signals. The FPGA is responsible for generating the proper timing to control the ASIC's acquisition cycle. An "Or-Out" signal is generated by the ASIC to indicate that one its channels has triggered. When the "Or-Out" goes active, the FPGA generates control and timing signals to command the ASIC to integrate the analog PSD input (i.e., the three windows). The integrated values are then digitized under control of the FPGA which stores the information in first-in-first-out (FIFO) memory until the processor reads it. The size of this FIFO is the "bottleneck" in the electronics chain, which may fill and limit the CAREE instrument to a maximum rate of about 20 kHz.These steps are repeated for each triggered channel during this event; the FPGA then generates a force-reset to command the ASIC to return to a "ready" mode, where it awaits another trigger.

For data transfer, a micro-USB port enables serial over USB communications with a PC. Alternatively, Ethernet is also available. The entire system is powered via power-over-Ethernet, the latter option provides the capability for a single tether (i.e., a CAT5 cable) during normal use. A TTL signal is delivered via LEMO; the digital pulse indicates a neutron event and is useful for simple interface with counting electronics. For direct communication with the user, a backlit LCD screen indicates count rates and other useful configured information.

The electronic assembly is divided into five custom-designed printed circuit boards (PCBs, see Fig.3). One card contains an EMCO Q15-CT high voltage power supply (HVPS) and active voltage divider for a Hamamatsu R6231

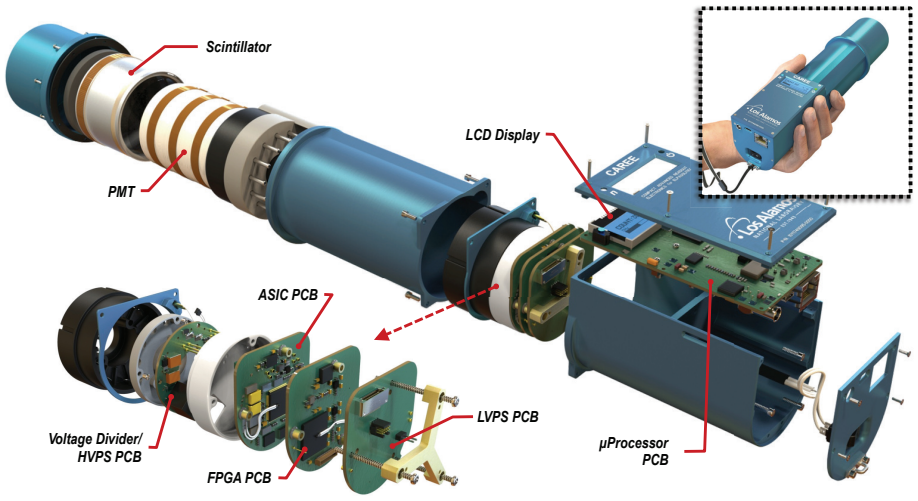

Figure 3: An exploded render of the CAREE instrument shows the major components and electronic boards. Inset: The instrument in use.

2"-diameter photomultiplier tube (PMT). A second card contains the ASIC front end electronics, including the PSD8C and thresholding and digitization components. Another board contains an Actel Igloo AGL1000-FG256 FPGA, ASIC interface, and data buffer. Finally, a low voltage power supply (LVPS) PCB provides a DC/DC conversion to enable the use of power over Ethernet (PoE). These four boards are all stacked and separated by standoffs in order to minimize volume.

The remaining board contains an ARM-9 microprocessor, and is largely based off the commercially available NXP LPC3250 with some key additions. Notably, the board contains a Sitronix ST7565R 65x132 dot matrix back-lit LCD, Ethernet connector for power and communication, micro-USB port for communication, LEMO port for neutron-indicating TTL-out, status LEDS, and a micro-SD card slot; the SD card is used to store the embedded software and configuration file, and for optional writing of data. Due to the size and mechanical considerations involving flush fitting of the LCD, this card sits adjacent to the stack.

The average current draw is 50.8 mA at 45.05 V, resulting in 2.28 W. At

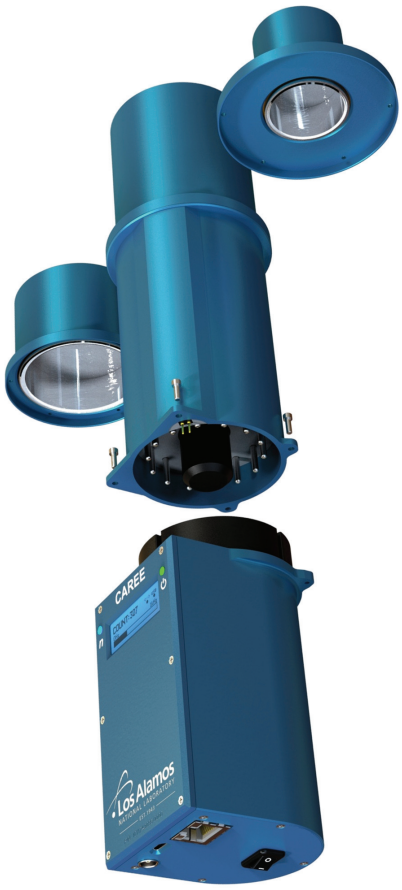

Figure 4: A mechanical render shows the separation of the electronic housing from the detector housing. Interchangeable modules allow for a variety of crystal sizes to be attached.

peak, however, the current may reach 67.4 mA (3.04 W). Since USB 2.0 is only rated to 2.5 W, this power draw explains why we opted to use PoE rather than USB power. However, the newer USB 3.0 standard supplies up to 4.5 W, which would suffice.

4. Mechanical

Mechanical design was motivated by the need for a compact, handheld instrument capable of modular interchange of multiple elpasolites and mated

PMTs. An aluminum electronics enclosure houses all five electronics boards using an extruded "mousehole" shape. On its flat face is the LCD, power LED, and an LED for indication of neutron events (this LED is tied to the TTL signal described in Sec. 3). The LEMO, micro-USB, and Ethernet port are located on the back face alongside a power switch. The front face contains a standard socket for interface with the Hamamatsu R6231 PMT. The electronics housing maintains a considerable volume of unused space; follow-on efforts will have the option to utilize the same mechanical design and include additional electronics for new capabilities.

The modularity of the design is made apparent by the description of the PMT/detector module; it consists of the housed scintillator mated to the PMT, and positioned within an aluminum housing. A channel on the side of the housing allows for a thermistor cable to run up its side. The thermistor is bonded to the top of the PMT as close to the scintillator as is feasible. This module provides both the mechanical and optical containment such that it can be easily swapped on an electronics module. Furthermore, as shown in Fig. 4, multiple size scintillator caps were developed to allow for a range of crystal sizes.

As designed and built, the handheld dimensions and overall mass depend on the crystal used, but assuming a housed 2"-diameter $\times$ 1.25"-long scintillator, CAREE has a mass of 958 g (the majority of which is the crystal) and measures 10.17" long, 2.22" wide, and 2.79" tall. The instrument is light enough to be easily handled, and the extruded "mousehole" design lends itself well to a hand contour.

5. Software

CAREE utilizes custom C-based embedded software for onboard data analysis, calibrations, corrections, data transfer, and commanding. Upon bootup, the microcontroller reads the embedded software binary from the micro SD card; this deliberate design decision eases the process for software updates since the operator may simply overwrite the binary file with a newer version. The em-

bedded code reads in the configuration parameters (more than 70 in total) from an ascii configuration file also located on the SD card, setting the appropriate registers. When interfaced with a PC, the user may read back, set, and store (i.e., write to the configuration file) these values.

For every event, each of the three integrated ADC values are pulled from the ASIC. Depending on the mode of operation, these raw values may be sent out directly ("list" mode), or else partially analyzed on-board. In the latter "spectral" mode, the PSD ratio is calculated, and total integration values converted to energy. The embedded software performs PSD, separating neutrons from gamma events in real time by thresholding the PSD ratio and energy to select a user-specified window specific to the expected output of a particular elpasolite. Gammas and thermal neutrons are thus packaged in their own spectra before being sent out to the external PC. Additionally, the embedded software reads analog-to-digital converters in order to measure specific state of health (SOH) values (including temperatures and voltages levels), and commands digital-to-analog converters in order to control offsets, gains, thresholds, and windows (within the ASIC).

The embedded software features a robust feature set in order make the instrument fieldable. Namely, a calibration routine allows for a ^{137}Cs source along with a force-trigger "zero" energy integration to be used to establish linear conversion values. Furthermore, a thermal stabilization routine [6] queries thermistors embedded on the ASIC and scintillator housing and corrects for temperature variabilities in both the scintillator and electronics. Signal offsets, gain (due to both scintillator and electronic thermal dependencies), and PSD are corrected within an ANSI standard temperature range of -20 to $+50^{\circ}$ C. We have previously shown such a routine to be necessary with CLYC scintillator due to thermal dependence of all scintillation mechanisms including those slower than CVL [1]; it follows that other elpasolites would demonstrate a similar thermal variance.

High-level analysis of the data is performed onboard a PC. A graphical user interface (GUI) uses a National Instruments Labview runtime engine and

Python code to communicate with the instrument via USB or Ethernet, parse incoming data, and display those data in real time. The GUI is capable of commanding and configuring the instrument by setting register values dealing with high voltage levels, discriminator thresholds, base offsets, energy conversion parameters, timing information, data modes, time intervals, and other configurations. Data streamed from the unit is saved in its "raw" binary format, but also converted to the American National Standards Institute's National Standard Data Format for Radiation Detectors Used for Homeland Security (N42.42) [18]. This xml-based text file allows for the data to be subsequently read by a number of standard interpreters, and is increasingly becoming a necessity in detectors developed for the United States Department of Homeland Security.

6. Preliminary Results

A total of twelve instruments (ten deliverables and two spares) were fabricated and optimized at Los Alamos National Laboratory. An example of a functioning unit is shown in Fig. 5. In the ten deliverables, only CLYC crystals were utilized: three 2"-diameter × 1.25"-long, and seven 1"-diameter × 1"-long. Following assembly, each of the ten units had offsets positioned, had thresholds optimized, were calibrated, and then were tested for resolution and basic performance. The results are listed in Table 1. Resolutions vary from about 5-7% (FWHM at 662 keV), a worse resolution than is achievable with CLYC. There are two primary reasons for the decreased resolution: the crystals are housed and not coupled directly to the PMT, and an optical pad mates the bare crystal to the housing window instead of epoxy. The former situation is necessitated by the modularity of the design; a direct mating would require a hygrosopic and semi-permanently enclosed PMT/scintillator housing. The latter fact is due to the need for the instrument to function over a temperature range defined by the ANSI standards for handheld detectors; a direct mating of the crystal to the housing glass would cause cracks in the crystal during thermal cycle due to a difference in thermal expansion coefficients between the window and crystal.

Figure 5: A photograph of CAREE in use. (A USB and Ethernet cable are both attached, although only the Ethernet is required.)

Electronic noise is also a factor in resolution measurement. Using the force trigger photopeak described in Sec. 5, a resolution degredation due solely to noise in the electronics may be determined. A Gaussian was fit to the "zero-energy" peak, and found to have a full width of 82 ADC units; with the gain and PMT used, this width corresponds to 13 keV, or 2.0% FWHM at 662 keV. At a measured resolution of the 662 keV photopeak of 6%, electronic noise thus accounts for about a 0.5% degredation in absolute resolution, a minor contribution. Despite less-than-optimal resolution, results for basic performance are as expected; a spectrum and PSD plot from a representative deliverable are shown in Fig. 6.

In order to derive the parameters required for the thermal stabilization routine, it was necessary to thermal cycle each of the ten units. All were placed in

Unit	Crystal Size (diam. x length)	Resolution (% FWHM @ 662 keV)
CAREE-01	2" × 1.25"	6.0
CAREE-02	2" × 1.25"	5.9
CAREE-03	2" × 1.25"	6.9
CAREE-04	1" × 1"	5.6
CAREE-05	1" × 1"	6.7
CAREE-06	1" × 1"	6.2
CAREE-07	1" × 1"	5.1
CAREE-08	1" × 1"	5.4
CAREE-09	1" × 1"	5.5
CAREE-10	1" × 1"	4.9

Table 1: Energy resolutions for each of the ten deliverable instruments (reporting FWHM at 662 keV).

a thermal chamber, connected to PoE switches, and placed on our institution's network. The chamber was cycled in 10° C increments between −20 and +50° C and soaked at that temperature. During the soak, data was acquired that was later used to derive the 9-parameter thermal stabilization routine as described in Sec. 5.

A test of the success of the thermal stabilization required two additional thermal cycles: one with the stabilization turned off, and one with it turned on. In each case the units were first calibrated, then the thermal chamber was cycled with all ten instruments using a ramp function from −20 to +50° C while continually acquiring data from both a ^{137}Cs and a moderated AmB source; no re-calibration took place during the cycle. Results are difficult to quantify since the measurements rely heavily on the ramp function used, and an apparent photopeak is not necessarily suitable for a Gaussian fit. However, we have generally seen improvements in energy resolution from about 8-12% when the thermal stabilization routine is disabled, to about 6-7% when enabled. Furthermore,

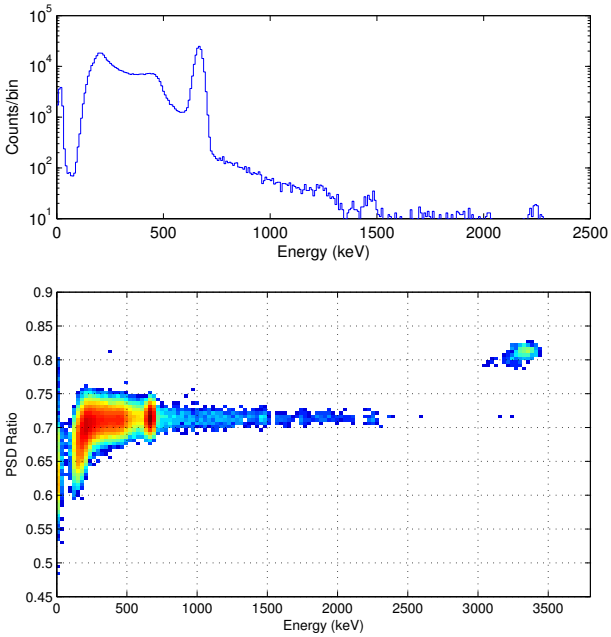

Figure 6: Data from a representative CAREE instrument shows (Top) A ^{137}Cs spectrum and (Bottom) a plot of PSD ratio versus energy.

neutrons typically fall outside of the window defined by PSD thresholds when the stabilization is disabled; when the routine is enabled, however, they remain correctly identified.

A true test of the instrument necessarily includes an evaluation of the scintillator. Following design and fabrication, our team ensured functionality of the electronics, capability of optimization, and success of the thermal stabilization routine. A comprehensive test is now being performed by a dedicated external team, which will evaluate the compatibility of the electronics with the scintillators provided.

7. Conclusion

Bromo- and Chloro-elpasolites are classes of inorganic scintillator that show promise in a dual-mode capability as gamma spectrometers and thermal neutron counters. The emission waveforms, which are dependent on the incident

particle, provide the possibility of pulse-shape discrimination, making feasible the separation of the two detection datasets. The large family of elpasolites includes crystals with various energy resolution, emission wavelengths, PSD performance, and density. In an effort to perform an efficient investigation into optimization of readout for any elpasolite, we developed the Compact Advanced Readout Electronics for Elpasolites. CAREE implements a suitable multi-window charge-integrating ASIC, custom PCBs, and a modular design feasible for use with most small-size housed elpasolite crystals. The system is handheld, portable, and easily commanded and read out by a PC GUI.

Ten deliverable units were fabricated, optimized, thermally-cycled, and tested for basic performance. We have reported results of resolution and thermal stabilization for CAREE instruments containing CLYC crystals. Analysis of these data have verified the optimization of the electronics, software, and configuration procedure. With establishment of the instrument and algorithms, future studies may now focus on other existing and in-development elpasolite scintillators.

Acknowledgement

This work was supported by the United States Defense Threat Reduction Agency through Interagency Agreements DTRA10027-5888-B and DTRA10027-7646-B.

References

[1] B. S. Budden, L. C. Stonehill, J. R. Terry, A. V. Klimenko, J. O. Perry, Characterization and investigation of the thermal dependence of $cs_2liycl_6:ce^{3+}$ (clyc) waveforms, IEEE Transactions on Nuclear Science 60 (2) (2013) 946–951.

[2] E. V. D. van Loef, J. Glodo, W. M. Higgins, K. S. Shah, Optical and scintillation properties of $cs_2liycl_6:ce^{3+}$ and $cs_2liycl_6:pr^{3+}$ crystals, IEEE Transactions on Nuclear Science 52 (5).

[3] D. W. Lee, L. C. Stonehill, A. Klimenko, J. R. Terry, S. R. Torngа, Pulse-shape analysis of cs_2liycl_6:ce scintillator for neutron and gamma-ray discrimination, Nuclear Instruments and Methods in Physics Research Section A 664 (2012) 1–5.

[4] B. Budden, A. Couture, L. Stonehill, A. Klimenko, J. Terry, J. Perry, Analysis of $cs_2liycl_6:ce^{3+}$ (clyc) waveforms as read out by solid state photomultipliers, in: Nuclear Science Symposium and Medical Imaging Conference (NSS/MIC), 2012 IEEE, 2012, pp. 347–350. doi:10.1109/NSSMIC.2012.6551123.

[5] M. B. Smith, M. McClish, T. Achtzehn, H. R. Andrews, M. J. Baginski, D. J. Best, B. S. Budden, E. T. H. Clifford, N. A. Dallmann, C. Dathy, J. M. Frank, S. A. Graham, H. Ing, L. C. Stonehill, "assessment of photon detectors for a handheld gamma-ray and neutron spectrometer using cs_2liycl_6:ce (clyc) scintillator, Nuclear Instruments and Methods in Physics Research Section A 715 (2013) 92–97.

[6] B. Budden, L. Stonehill, N. Dallmann, J. Michel, M. Baginski, D. Best, C. Dathy, J. Frank, M. McClish, M. Smith, Gain stabilization and pulse-shape discrimination in a thermally-variant environment for a hand-held radiation monitoring device utilizing $cs_2liycl_6:ce^{3+}$ (clyc) scintillator, in: Nuclear Science Symposium and Medical Imaging Conference (NSS/MIC), 2012 IEEE, 2012, pp. 351–356. doi:10.1109/NSSMIC.2012.6551124.

[7] B. S. McDonald, M. J. Myjak, W. K. Hensley, J. E. Smart, System modeling and design optimization for a next-generation unattended sensor, IEEE Transactions on Nuclear Science 60 (2) (2013) 1102–1106.

[8] J. Glodo, W. M. Higgins, E. V. D. van Loef, K. S. Shah, 'scintillation properties of 1 inch cs_2liycl_6:ce crystals,, IEEE Transactions on Nuclear Science 55 (3) (2008) 1206–1209.

[9] P. A. Rodnyi, Core-valence luminescence in scintillators, Radiation Measurements 38 (2004) 343–352.

[10] S. Mukhopadhyay, C. Stapels, E. B. Johnson, E. C. Chapman, P. S. Linsay, T. H. Prettyman, M. R. Squillante, C. F. James, Comparison of neutron sensitive scintillators for use with a solid-state optical detector, in: SPIE Proceedings, Vol. 7449, 2009.

[11] J. Glodo, E. van Loef, R. Hawrami, W. M. Higgins, A. Churilov, U. Shirwadkar, K. S. Shah, Selected properties of cs_2liycl_6, $cs_2lilacl_6$, and $cs_2lilabr_6$ scintillators, IEEE Transactions on Nuclear Science 58 (1).

[12] J. Glodo, R. Hawrami, E. van Loef, U. Shirwadkar, K. S. Shah, Pulse shape discrimination with selected elpasolite crystals, IEEE Transactions on Nuclear Science 59 (5) (2012) 2328–2333.

[13] M. B. Smith, T. Achtzehn, H. R. Andrews, E. T. H. Clifford, H. Ing, V. D. Kovaltchouk, Fast neutron spectroscopy using cs_2liycl_6:ce (clyc) scintillator, IEEE Transactions on Nuclear Science 60 (2) (2013) 855–859.

[14] J. Glodo, U. Shirwadkar, R. Hawrami, T. Achtzehn, H. R. Andrews, E. T. H. Clifford, H. Ing, V. D. Kovaltchouk, M. B. Smith, K. S. Shah, Fast neutron detection with cs_2liycl_6, IEEE Transactions on Nuclear Science 60 (2) (2013) 864–870.

[15] B. Budden, L. Stonehill, N. Dallmann, M. Baginksi, D. B. M. Smith, S. Graham, C. Dathy, J. Frank, M. McClish., A cs_2liycl_6:ce-based advanced radiation monitoring device, IEEE Transactions on Nuclear Science 784 (2015) 97–104.

[16] U. Shirwadkar, R. Hawrami, J. Glodo, E. Van Loef, K. Shah, Novel scintillation material $cs_2lilabr_6 - Xcl_x$:ce for gamma-ray and neutron spectroscopy, in: Nuclear Science Symposium and Medical Imaging Conference (NSS/MIC), 2012 IEEE, 2012, pp. 1963–1967. doi:10.1109/NSSMIC.2012.6551453.

[17] G. L. Engel, M. J. Hall, J. M. Proctor, J. M. Elson, L. G. Sobotka, R. Shane, R. J. Charity, Design and performance of a multi-channel, multi-

sampling, psd-enabling integrated circuit, Nuclear Instruments and Methods in Physics Research Section A 612 (1) (2009) 161–170.

[18] Ansi n42.42-2012 (revision of ansi n42.42-2006), American National Standard Data Format for Radiation Detectors Used for Homeland Security.